

A PRELIMINARY STUDY FOR THE COUPLED ATMOSPHERE-STREAMFLOW MODELING IN KOREA

Deg-Hyo Bae¹, Jun-Seok Chung², and Won-Tae Kwon²

1. Department of Civil Engineering, Changwon National University, Kyongnam, Korea

2. Meteorological Research Institute, Seoul, Korea

Abstract: This study presents some results of a preliminary study for the coupled precipitation and river flow prediction system. The model system is based on three numerical models, Mesoscale Atmospheric Simulation model for generating atmospheric variables, Soil-Plant-Snow model for computing interactions within soil-canopy-snow system as well as the energy and water exchange between the atmosphere and underlying surfaces, and TOPMODEL for simulating stream flow, subsurface flow, and water table depth in a watershed. The selected study area is the 2,703 km² Soyang River basin with outlet at Soyang dam site. In addition to providing the results of rainfall and stream flow predictions, some results of DEM and GIS application are presented. It is obvious that the accurate river flow predictions are highly dependant on the accurate precipitation predictions.

Key Words. MAS model, TOPMODEL, coupled modeling system, Soyang River basin

1. INTRODUCTION

It has been developed many hydrological rainfall-runoff models for flood prediction. They are generally composed of a surface runoff component and a stream-channel, or a reservoir routing component. Those predictive models, however, are not suitable for the real-time short-term flood prediction system because they require observed precipitation information before they make river flow predictions. In most cases, by the time rainfall is observed, there is very little time left for any decision makings of flood warning. In this sense, rainfall forecasts in time advance are indispensable and a coupled atmosphere-river flow forecasting system is essential for the reliable flood forecasting

system.

Since the computerized flood forecasting system in Korea was introduced in 1974 at the Han River Flood Control Center (FCC), several different types of rainfall-runoff model have been used for the various water resources management practices. The typical ones are: the rational formula, unit hydrograph, Kajiyama formula, and TANK model for the water resources planning and design; HEC-1, HEC-2, SSARR, SWM, SWMM. Storage Function Method (SFM) for the flood analysis. The lumped conceptual SFM for both watershed and channel routing developed by Kimura (1961) has been used to predict the floods in the main FCCs. This model is based on the conservation of mass with relationship that storage of a conceptual

reservoir is a nonlinear function of outflow. This method has an advantage that the computation procedures are relatively simple, but has a disadvantage that it can only compute the flows for a single event. Several scientists were tried to test more complicated physically-based models such as HEC-1 model and SSARR model on the Han River basin. They temporally concluded that those models are inadequate to use on the basin due to the complication of model parameters and lacks of hydrological and geologic data, and decided that the storage function methods for both watershed and channel routing are used (MOC, 1987). In addition, it has no chance to make river flow predictions using the rainfalls predicted from atmospheric numerical models.

The purpose of this study is to provide some results of a preliminary study for the coupled precipitation and river flow prediction system. The model system is composed of three numerical models, Mesoscale Atmospheric Simulation (MAS) model for generating atmospheric variables, Soil-Plant-Snow (SPS) model for computing interactions within soil-canopy-snow system, and TOPMODEL for simulating stream flow, subsurface flow, and water table depth in a watershed. It is apparently the first time that the coupled model between atmosphere and river flow is tested on the hydrologic watershed scale in Korea.

2. DESCRIPTION OF ATMOSPHERE-STREAMFLOW MODEL

The model used in this study is the Coupled Atmosphere-River Flow Simulation (CARS) system, which is composed of three numerical models, a Mesoscale Atmospheric Simulation (MAS) model, a Soil-Plant-Snow

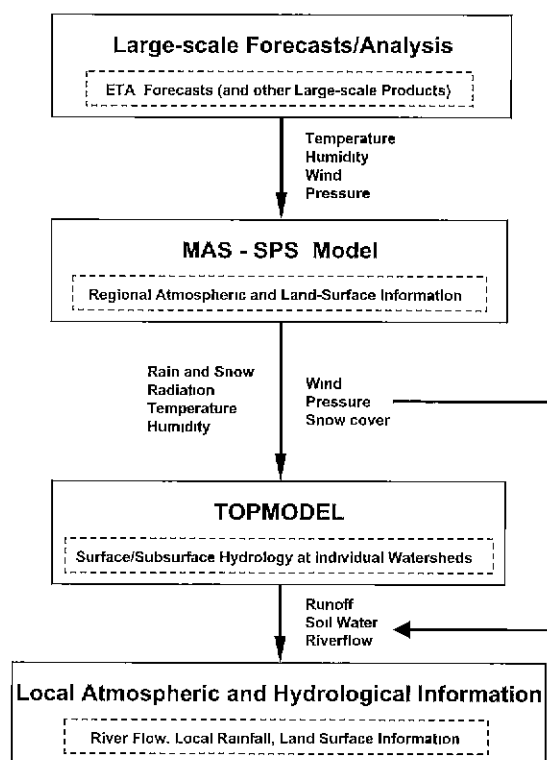


Fig. 1. Nesting Procedure of CARS System

(SPS) model, and TOPMODEL. Fig. 1 represents the nesting procedure of the CARS system. The MAS and SPS models are interactively coupled sharing the same horizontal mesh, while the TOPMODEL is imposed on individual watershed. As illustrated in Fig. 1, because the CARS system can be nested within either a large-scale forecast or analysis data, the system may be employed for predictions of regional climatology depending on the choice of the large-scale input data. A brief description of dynamics, physics, and numerical features of each model component are as follows:

2.1 MAS Model

The governing equations of MAS model

for simulating regional atmospheric and land-surface processes are the flux form of the primitive equation written on σ -coordinates (Soong and Kim, 1996).

$$\begin{aligned} \frac{\partial(\pi u)}{\partial t} = & -m^2 \left[\frac{\partial}{\partial x} \left(\frac{\pi uu}{m} \right) + \frac{\partial}{\partial y} \left(\frac{\pi vu}{m} \right) \right] \\ & + \pi (f + \gamma) v - \frac{\partial(\pi \sigma \bar{u})}{\partial \sigma} \\ & - m \left(\frac{\partial \phi}{\partial x} - \sigma \frac{\partial \phi}{\partial \sigma} \frac{\partial \sigma}{\partial x} \right) + \pi F_x \end{aligned} \quad (1)$$

$$\begin{aligned} \frac{\partial(\pi v)}{\partial t} = & -m^2 \left[\frac{\partial}{\partial x} \left(\frac{\pi uv}{m} \right) + \frac{\partial}{\partial y} \left(\frac{\pi vv}{m} \right) \right] \\ & + \pi (f + \gamma) u - \frac{\partial(\pi \sigma \bar{v})}{\partial \sigma} \\ & - m \left(\frac{\partial \phi}{\partial y} - \sigma \frac{\partial \phi}{\partial \sigma} \frac{\partial \sigma}{\partial y} \right) + \pi F_y \end{aligned} \quad (2)$$

$$d\phi = -C_p \theta dP \quad (3)$$

$$\begin{aligned} \frac{\partial(\pi \theta)}{\partial t} = & -m^2 \left[\frac{\partial}{\partial x} \left(\frac{\pi u \theta}{m} \right) + \frac{\partial}{\partial y} \left(\frac{\pi v \theta}{m} \right) \right] \\ & - \frac{\partial(\pi \sigma \bar{\theta})}{\partial \sigma} + \pi Q \end{aligned} \quad (4)$$

$$\begin{aligned} \frac{\partial(\pi q)}{\partial t} = & -m^2 \left[\frac{\partial}{\partial x} \left(\frac{\pi u q}{m} \right) + \frac{\partial}{\partial y} \left(\frac{\pi v q}{m} \right) \right] \\ & - \frac{\partial(\pi \sigma \bar{q})}{\partial \sigma} + \pi S \end{aligned} \quad (5)$$

$$\frac{\partial \pi}{\partial t} = -m^2 \left[\frac{\partial}{\partial x} \left(\frac{\pi u}{m} \right) + \frac{\partial}{\partial y} \left(\frac{\pi v}{m} \right) \right] - \frac{\partial(\pi \sigma \bar{\sigma})}{\partial \sigma} \quad (6)$$

$$\gamma = -v \frac{\partial m}{\partial x} + u \frac{\partial m}{\partial y}$$

where m is the map factor, $\pi = p_{\text{slc}} - p_{\text{top}}$, $P = (p/p_0)^{R_d/C_p}$, Q is the diabatic heating rate, and S is the net source/sink of a tracer variable q such as water vapor, condensed water, and other pollutants, and F_x and F_y are non-conservative forcing on the x - and

y -component of momentum, respectively. The curvature term γ is much smaller than the Coriolis parameter in middle latitudes and may be neglected.

This model includes the advection scheme by Takacs (1985), Hsu and Arakawa (1990). The scheme is characterized by third-order accuracy in time and space, near positive-definiteness with negligible phase error, and minimal numerical oscillation. Such numerical characteristics of the advection scheme provide a significant advantages for simulating atmospheric flows over complex terrain and with strong physical forcing. The MAS model includes a quite complete set of physics such as an explicit microphysics scheme and multi-level solar- and terrestrial radiative transfer that the effects of clouds.

2.2 SPS Model

The SPS model (Kim and Ek, 1995) is a modified version of the coupled atmosphere plant snow (CAPS) model developed by Mahrt and Pan (1984) and Ek and Mahrt (1991). It computes interactions within a soil-canopy- snow system as well as the energy and water exchange between the atmosphere and underlying surfaces. The governing equations for the volumetric soil water content and soil temperature of a given soil layer can be written as

$$C(Q) \frac{\partial T}{\partial t} = \frac{\partial}{\partial z} \left[K_T(Q) \frac{\partial T}{\partial z} \right] + F_T \quad (7)$$

$$\frac{\partial Q}{\partial t} = \frac{\partial}{\partial z} \left[K_Q(Q) \frac{\partial Q}{\partial z} \right] + \frac{\partial D(Q)}{\partial z} + F_Q \quad (8)$$

where $C(Q)$ is the volumetric soil heat capacity, $K_T(Q)$ is the soil heat conductivity, $K_Q(Q)$ is the soil moisture

diffusivity, and $D(Q)$ is the hydraulic conductivity of a soil layer. The terms F_T and F_Q represent source and sink terms for soil temperature and soil water content, respectively. On the other hand, the canopy water content (W_c) is computed by

$$\frac{\partial W_c}{\partial t} = P - D_r - E_c \quad (9)$$

where P is the precipitation rate, D_r is the rate of water dripping from the canopy on to the ground, and E_c is the evaporation of the canopy water.

2.3 TOPMODEL

The TOPMODEL is a watershed model that simulates stream flow, subsurface flow, and the water table depth in a watershed. The basic concepts of the model are proposed by Kirkby and coded by Beven (Beven et. al., 1994). One of the characteristics of the model is that the modeling concepts have been kept simple enough so that the model structures can be easily modified to bring the results closer to the modeler's perceptions for the behaviors of a particular catchment. From this reason, there exist many different types of the model, but the main components of the model are topographic index distribution component, soil water change component, surface runoff and channel routing component.

The starting points used to derive the fundamental TOPMODEL equations are the assumptions that (1) the dynamics of the saturated zone can be approximated by successive steady state representation, (2) the hydraulic gradient of the saturated zone can be approximated by the local surface

topographic slope, and (3) the saturated hydraulic conductivity decreases exponentially with soil depth. From these three assumptions, one fundamental equation that represents the relationship between the watershed average groundwater depth \bar{z} and water table depth z_i at any location i is given as:

$$f(\bar{z} - z_i) = \left[\ln \frac{a}{\tan \beta} - \frac{1}{A} \sum_i \ln \frac{a}{\tan \beta} \right] - \left[\ln T_0 - \frac{1}{A} \sum_i \ln T_0 \right] \quad (10)$$

where, f is a parameter related to the rate of change of saturated hydraulic conductivity with depth, a is the upslope area per unit contour length at any location, $\tan \beta$ is the gravitational gradient at the location. The first and second terms of right hand side in Equation (10) denote the topographic index and basin averaged topographic index, respectively. Equation (10) is applied to every point i to determine the location and extent of saturated land surface areas, indicated by points where $z_i \leq 0$. The fraction of the saturated area, which is called as contributing area, gives direct surface runoff. On the other hand, total subsurface flow Q_b is computed as:

$$Q_b = \left(\frac{K_0}{f} \right) e^{-\lambda} \cdot e^{-f\bar{z}} \quad (11)$$

where K_0 is the saturated hydraulic conductivity at the surface. Equation (11) shows that the mean value of the topographic index λ is inversely related to the potential rate of subsurface flow. It means that watershed with high λ values have low potential subsurface flow rates. A typical example watershed with high λ value is gentle slope area.

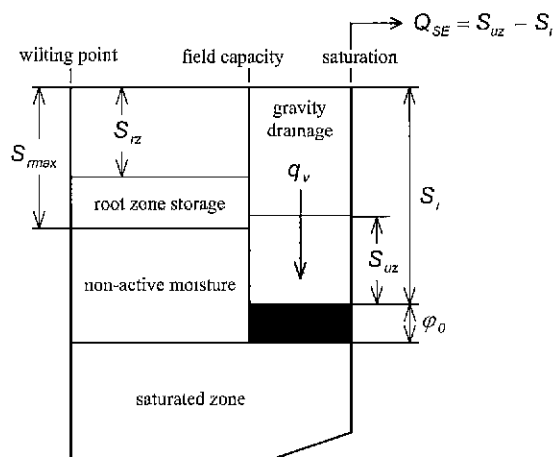


Fig. 2. Soil Water Variation in TOPMODEL

As it can be seen in Equation (10), all locations with the same topographic index are hydrologically similar under the assumption that T_0 , lateral transmissivity when the soil is just saturated, is equivalent to all grid points in a watershed. It allows the aggregation of the topographic index distribution from a spatially explicit description of the watershed into one composed of intervals of $\ln(a/\tan \beta)$. Fig. 2 shows the schematic diagram for soil moisture variation at each topographic index interval. As it can be seen in the figure, the model has two soil layers: unsaturated zone and saturated zone. The soil water contents in an unsaturated zone are varied on the range of zero to saturation point via wilting point and field capacity depending on precipitation inflows, evaporation outflows, and gravity drainage from unsaturated zone to saturated zone. The overland flows that occur the unsaturated zone is filled are routed by the use of a distance-related delay (Beven and Kirkby, 1979).

3. CASE STUDY

The study area is the Soyang River

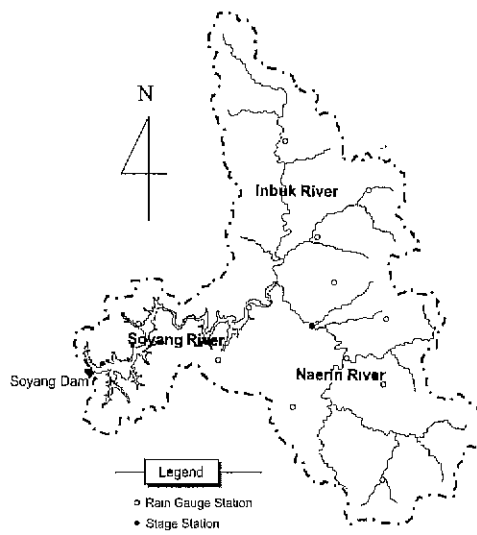


Fig. 3. Study area

drainage basin, which is the largest tributary of the North Han River, located in east central Korean peninsula. It is located approximately 85 km northeast of Seoul, Korea and the boundary of the basin is within approximately 127.8° E to 128.6° E in longitude and 37.7° N to 38.5° N in latitude. The area of the drainage basin is $2,703 \text{ km}^2$ with outlet at Soyang Dam site, as shown in Fig. 3. The Soyang River starts from the Odae Mountain at an altitude of about 1,560m. It flows southwesterly to the junction with the North Han River near the Chunchen City. The Soyang river is a main source of inflow into the Soyang dam, located in Soyang river 12km upstream from the junction, which has a storage capacity of $9,600,000 \text{ m}^3$ with 123m height and 530m length. Most of the terrain consists of mountain covered by coniferous and deciduous forests.

For the simulation of regional atmosphere and land-surface processes, the 18-layer version of the MAS model is utilized in this

study. The dependence variables are staggered on the Arakawa-C grid and the Lorenz grid (Lorenz, 1960) horizontally and vertically, respectively. The model domain for the MAS-SPS is $5,400\text{km} \times 4,800\text{km}$ with a $60\text{km} \times 60\text{km}$ resolution on a Lambert Conformal map projection. The main area of interest in this study is within and near the Soyang River basin in Korean peninsula. One of the crucial requirements for regional hydroclimate simulation is a data base to provide land surface characteristics. The SPS model requires soil texture, green-leaf fraction (GLF), leaf-area index (LAI), and vertical distribution of root density. The coupled MAS-SPS model also needs spectral albedo, roughness length, and zero-displacement height as a function of vegetation type. The soil texture provided by Zobler (1986) is used. The GLF and LAI are obtained from the monthly-mean values for Gutman and Iganov (1977) and the NASA/GSFC DACC (1995), respectively. Due to the lack of data, it is assumed that vegetation root density is uniform through the model soil layers.

NCEP (National Center of Environmental Prediction, USA) reanalysis data of which resolution is $2.5^\circ \times 2.5^\circ$ was interpolated to $60\text{km} \times 60\text{km}$ grids by Barnes scheme. Initial conditions and time-dependant lateral boundary conditions were provided from this data set. The reanalysis surface data are used to obtain initial conditions of soil temperature and soil moisture content. The lateral boundary conditions were provided every 6 hours from the NCEP reanalysis data. Fig. 4 shows the simulated daily-total precipitation within the MAS-SPS model run domain for the period of August 23, 01:00 to August 27, 24:00, 1995. To evaluate the simulated precipitations, it needs to compare grid-point

values against raingauge data within the grid points. However, grid-point values are not directly comparable to a raingauge data since the area presented by a grid point and a raingauge are different by many orders of magnitude. Therefore, the comparison of area-mean and time-mean values of the observed and simulated precipitation will be possible. With the observed and simulated river flows in the study area, the comparison and evaluation of predicted precipitation are followed later.

Before the coupled atmosphere-streamflow system is used for the application of various water resources managements, the model parameters in TOPMODEL must be estimated from historical meteorological and hydrological data, and from all available catchment information. The required model inputs are MAP (mean areal precipitation) and potential evapotranspiration (or pan evaporation). The river flows are optionally needed for the model calibration and verification. As it can be seen in Fig. 3, the study area has several precipitation and stage stations for the hydrological and meteorological variables. The MAPs are computed from the records of all 12 stations in and near the basin using the Thiessen's weighted average method. The potential evapotranspiration data from the Chuncheon meteorological station are used. The inflows for the Soyang dam are used for the river flow data at the river basin outlet. The manual estimation technique is used for the estimate of TOPMODEL parameter using the event during May 1~October 31, 1990 (hereafter called 1990 event). Table 1 shows the meanings and estimated model parameters in the study area. One of the characteristics of TOPMODEL run is required a distribution

95 AUG 23-28 PRECIPITATION

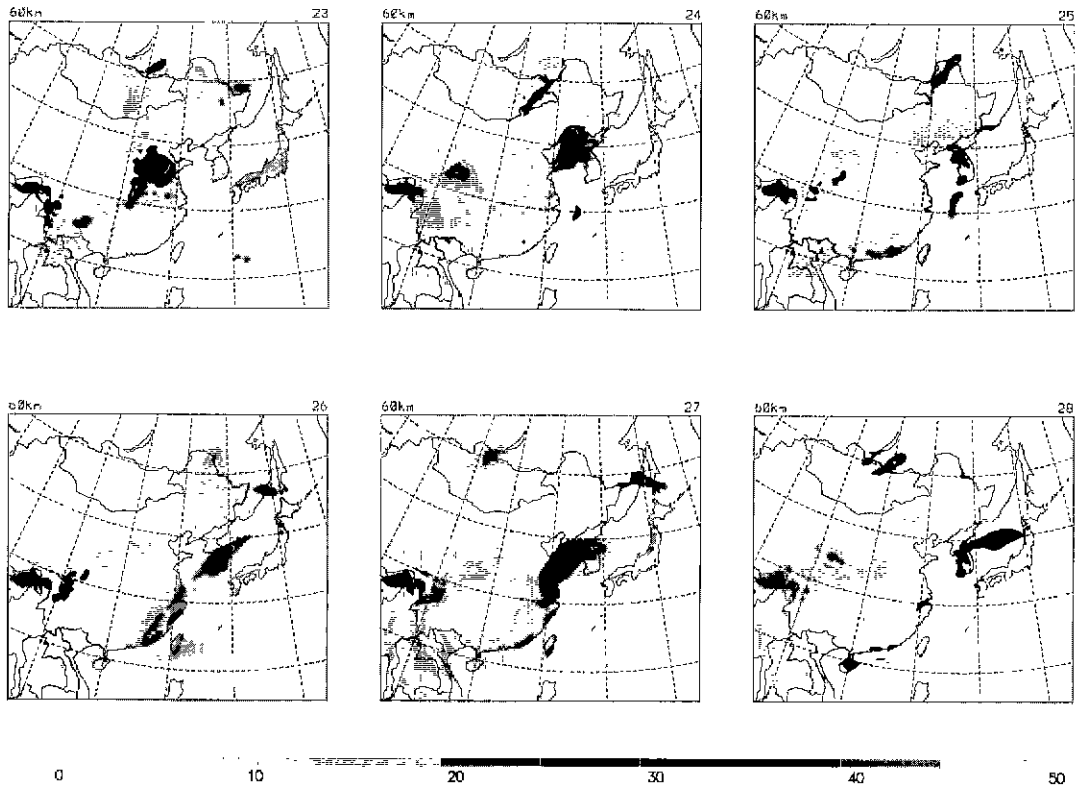


Fig. 4. The Simulated Daily-Total Precipitation

Table 1. Description and Estimates of the TOPMODEL Parameter

symbol	Description [unit]	Value
m	transmissivity recession coefficient with depth[m]	50.0
T_0	saturated lateral transmissivity[$\ln(m^2/hr)$]	0.208
S_{rmax}	maximum allowable storage deficit of root zone[m]	25.0
t_d	time delay coefficient in unsaturated zone[hr]	0.087
ν	internal and main channel routing velocity[m/hr]	5,500

of topographic index for the study area. These values can be computed from 3" DEM data. Fig. 5 shows the computed distribution of topographic index in the Soyang River basin. This distribution is obtained from the grid-point topographic index values on each

3" grid interval within the study area as shown in Fig. 6. The values of the topographic index are ranged on 1.96~17.47 and the maximum frequency is 0.154 at the value of 5.70.

Fig. 7 represents the observed and

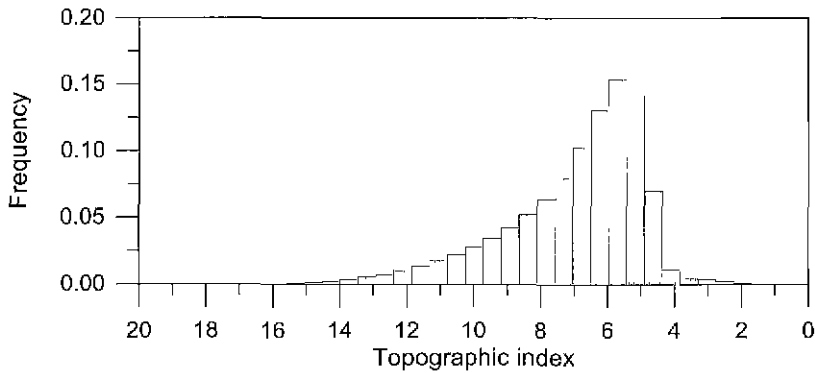


Fig. 5. Frequency Distribution of Topographic Index in the Soyang River Basin

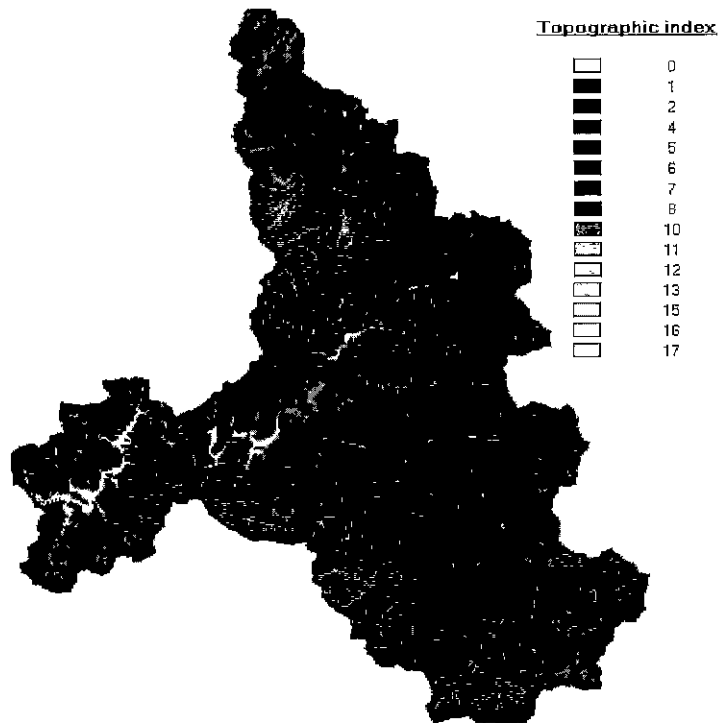


Fig. 6. Grid-point Values of $\ln(a/\tan \beta)$ within the Study Basin

computed discharges corresponding to the observed rainfall and evapotranspiration for the 1990 event. The rainfalls are MAPs computed from the weighted average method. The flood event on September 12, 01:00, 1990 (refer to time step 135) at Soyang dam

site is reached close to EL. 197.99m, which is the highest stage since the dam has been constructed. It was caused by two consecutive rainfall events of 402.3 mm during September 9 to 11, 1990. When the computed flows are compared with the

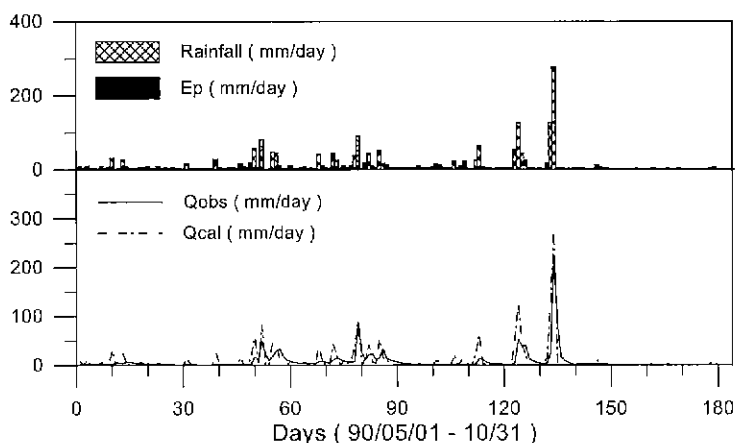


Fig. 7. The Observed and Simulated Flows at Soyang Dam Site (1990 Event)

observed ones, it can be seen that the observed flows and computed flows are well agreed.

Fig. 8 shows the sensitivity of river flows depending on the accuracy of rainfall estimates for the period of August 23, 01:00~August 27, 24:00, 1995 (hereafter called 1995 August event). As it can be seen in this figure, the sensitivities are tested on 4 different steps: the first step is the previous time period of rising limb of hydrograph, the second the period of rising limb of hydrograph, the third the period of near the peak flow, and the fourth the period of decreasing limb of hydrograph. The flows are computed under the condition that rainfalls at each step are perturbed to $\pm 50\%$, $+100\%$ of the original rainfalls. Table 2 shows the variation of volume flows depending on rainfall estimates. When the relative errors for the computed river flows between before and after rainfall perturbation are compared, the first step is the most sensitive under the same perturbing ratio. This is mainly caused that the under/overestimation of the rainfall on the first step will be critical to the variation of soil water content, which is

directly related to the amount of surface runoff and river flow. It is also interesting that the overestimation of rainfall causes higher river flow errors than underestimation of rainfall, when the simulated river flows according to $\pm 50\%$ change of rainfall prediction are compared. This phenomenon is especially dominant on the third step, because the status of soil water content near the peak hydrograph are mostly saturated and, therefore, the additional rainfall due to overestimation of rainfall near the peak flow is directly contribute to river flow. It can be seen that the accurate prediction of precipitation during the previous time step of flood hydrograph is important for the accurate prediction of discharge hydrograph and the magnitude of peak flow is highly affected by the amount of precipitation near the peak flow.

Fig. 9 shows the operational forecasts of precipitation and river flow for the 1995 August event. The "Robs" in the Figure represents the MAP computed from 13 station precipitation records within the basin, while "Rcal" denotes the predicted precipitation obtained from the MAS model

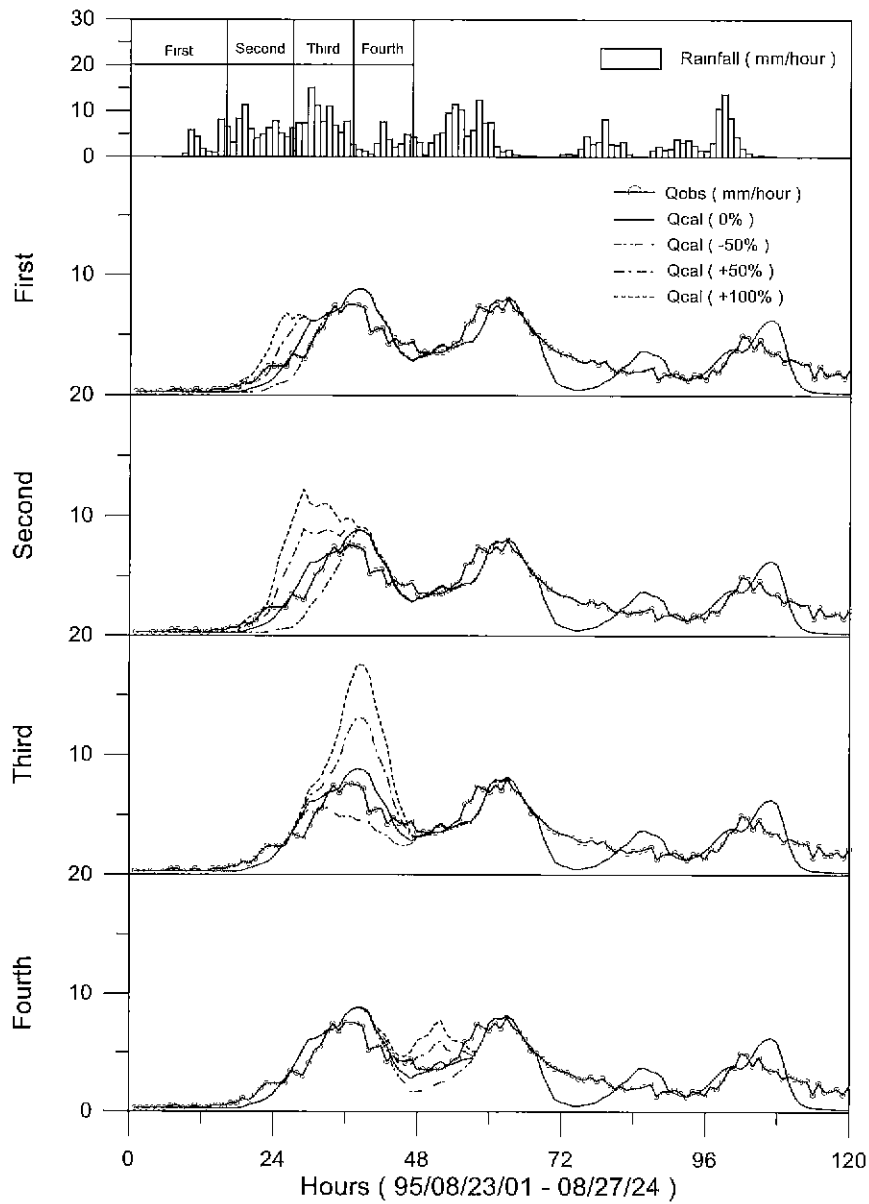


Fig. 8. Sensitivity of River Flow Depending on the Accuracy of Precipitation Prediction

Table 2. Variation of Volume Flows According to Rainfall Changes

Step	Variables Rainfall	Volume Flows according to Rainfall Change				Remark
		0%	-50%(Error)	+50%(Error)	+100%(Error)	
1	29.59	63.14	49.62(-21.4%)	77.85(+23.3%)	91.95(+45.6%)	
2	67.94	208.14	178.05(-14.5%)	245.96(+18.2%)	280.07(+34.6%)	
3	82.50	202.84	171.43(-15.5%)	253.98(+25.2%)	295.34(+45.6%)	
4	31.88	103.00	86.93(-15.6%)	118.89(+15.4%)	134.78(+30.9%)	

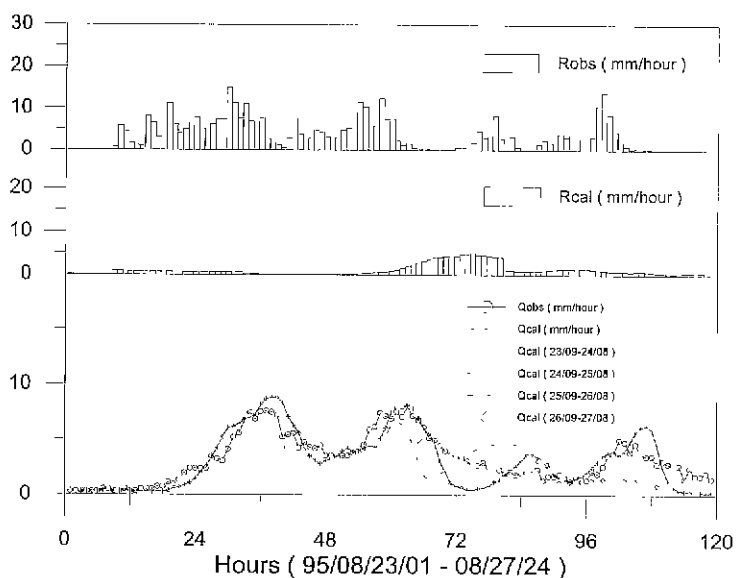


Fig. 9. Operational Forecasts of Precipitation and River Flow for 1995 August Event

run. In this study, two grid points (grid-point on 37.55°N , 128.19°E and point on 38.09°N , 128.20°E) are existed in and near the study area on the 60-km grid scale. Model runs are renewed on every 9 a.m. for the 48-hour precipitation forecast. In other words, from the initial climatic condition at 9 a.m. of t -day, the computations of next 48 hours upto 8 a.m. of $(t+2)$ -day are performed on hourly time step, and then predicted precipitations ("Rcal" in the figure) from 9 a.m. of $(t+1)$ -day to 8 a.m. of $(t+2)$ -day are taken for the next day 24-hr predicted precipitations. For the convenience, the first step is 24-hr period starting from 9 a.m. of 23rd; the second, the third, and the fourth steps are also 24-hr period starting from 9 a.m. of 24th, 25th, and 26th, respectively. The predicted precipitation from the MAS model on each time step is 16.95, 4.6, 76.2, and 25.35 mm, while the observed precipitation on the same time step is 146.23, 118.09, 64.76, 73.36 mm, respectively. It can

say that the computed precipitations are much less than the observed ones during 1995 August event. This is mainly caused that, on the model simulation, the rain band passed the upper area of the study area, as it can be seen in Fig. 4. This is a case that frequently happen for the precipitation prediction simulation. In this case study, it can say that the qualitative precipitation predictions are more or less successful, but the quantitative precipitation predictions are much underestimated. The "Qobs" in the legend represents the observed flow at the Soyang dam site, while the "Qcal" denotes the computed hydrograph using the predicted precipitations obtained by MAS model run. The volume flow obtained from the observed precipitation during the event is 389.70 mm, while that from the predicted rainfall at each step is 242.94, 258.70, 383.61, and 324.16 mm, respectively. It is obvious that accurate and timely predictions of precipitation are crucial for the accurate flow predictions.

4. SUMMARY AND CONCLUSIONS

This study provided the results from atmosphere-stream flow coupling study in Korea. The used model system is composed of MAS model, SPS model and TOPMODEL. The MAS model simulates precipitation and atmospheric variables at a 60-km horizontal resolution using initial and time-dependent lateral boundary conditions obtained from large-scale atmospheric input data. The simulated precipitation and atmospheric variables are then averaged over the Soyang River basin. TOPMODEL computes river flow using the watershed area mean precipitation and atmospheric variables simulated by MAS model. Some important results obtained from this study are summarized as follows. The topographic index values computed from 3" DEM data in the study area are ranged on 1.96~17.47 with the maximum frequency 0.154 at the value of 5.70. When the observed flows and model computed flows are compared on both daily- and hourly- time intervals, the TOPMODEL can successfully simulate the river flows in the study. As far as the river flow sensitivities depending on the accuracy of precipitation prediction, it can be seen that the accurate precipitation prediction during the previous time step of flood hydrograph is important for the accurate prediction of discharge hydrograph and the magnitude of peak flow is highly affected by the amount of precipitation near the peak flow. Also, for the operational forecasts of precipitation and river flow, it is obvious that the accurate and timely predictions of precipitation are crucial for the accurate flow predictions. In the future, we need to test the coupled model on various types of precipitation pattern. It is

also recommended that the coupled system tests on a uniform resolution 20km × 20km grid mesh in the horizontal.

ACKNOWLEDGEMENTS

This research was performed for the Natural Hazards Prevention Research Project, one of the Critical Technology-21 Programs, funded by the Ministry of Science and Technology of Korea.

REFERENCES

- Beven, K.J., and Kirkby, M.J. (1979). "A physically-based, variable contributing area model of basin hydrology." *Hydrological Sciences Bulletin*, 24(1), pp. 43-69.
- Beven, K., Quinn, P., Romanowicz, R., Freer, J., Fisher, J., and Lamb, R. (1994). *TOPMODEL and GRIDATB, A users guide to the distribution versions (94.03)*. CRES Technical Report TR110/94, Lancaster University, UK.
- Ek, M., and Mahrt, L. (1991). *OSU 1-D PBL Model User's Guide*. Dept. of Atmos. Sci., Oregon State Univ., Corvallis, OR, 118 pp.
- Gutman, F., and Ignov, A. (1997). "Derivation of green vegetation fraction from NOAA/AVHRR for use in numerical weather prediction models." *International J. Remote sensing*.
- Hsu, Y., and Arakawa, A. (1990). "Energy conserving and potential-entropy dissipating schemes for the shallow water equations." *Mon wea. Rev.*, 118, pp. 1960-1969.
- Kim, J., and Ek, M. (1995). "A simulation of the surface energy budget and soil water content over the Hydrologic

- Atmospheric Pilot Experiment-Modelisation du Nilan Hydrique forest site." *J. Geophys. Res.*, 100, D10, pp. 20845-20854.
- Kim, J., and Soong, S.-T. (1994). "Simulation of a precipitation event in the western United States." *Proceedings of the Sixth Conference on Climate Variations*, 23-28, January 1994, Nashville, TN, pp. 403-406.
- Kim, J., and Soong, S.-T. (1996). *Simulation of a precipitation event in the western United States*, Regional Impacts of Global Climate Change, Ed. Gahn, Rykiel, Pennell, Scott, Peterson, and Vail, 394pp.
- Kimura, T. (1961). *Flood runoff routing by storage function method*, Public Work Research Institute, Ministry of Construction, Japan.
- Lorenz, E.N. (1960). "Energy and numerical weather prediction." *Tellus*, 12, pp. 364-373.
- MOC (1987). *The Han River flood forecasting system*. Han River Flood Control Center, Ministry of Construction, Korea.
- Mahrt, L., and Pan, H.-L. (1984). "A two-layer model of soil hydrology", *Bound Layer Met.*, 29, pp. 1-20.
- Miller, N.L., and Kim, J. (1996). "Numerical prediction of precipitation and river flow over the Russian River watershed during the January 1995 California storms." *Bull. Am. Meteor. Soc.*, 77(1), pp. 101-110.
- Sivapalan, M., Wood, E.F., and Beven, K.J. (1990). "On hydrologic similarity, 3, A dimensionless flood frequency model using a generalized geomorphic unit hydrograph and partial area runoff generation." *Water Resources Research*, 26, pp.43-58.
- Soong, S.-T., and Kim, J. (1996). "Simulation of a heavy wintertime precipitation event in California." *Climate Change*, 32, pp. 55-77.
- Takacs, L. L. (1985). "A two-step scheme for the advection equation with minimized dissipation and dispersion errors." *Mon. Wea. Rev.*, 113, pp. 1050-1065.
- Wolock, D.M., and Hornberger, G.M. (1991). "Hydrological effects of changes in atmosphere carbon dioxide levels." *J. of Forecasting*, 10, pp. 105-116.
- Wood, E., Sivapalan, F.M., and Beven, K.J. (1990). "Similarity and scales in catchment storm response." *Rev. of Geophysics*, 28, pp.1-28.
- Zobler, L. (1986). *A world soil file for global climate modeling*, NASA Tech Memo. 87802.
-
- Deg-Hyo Bae, Department of Civil Engineering, Changwon National University, 9 Sarim-Dong, Changwon, Kyongnam, 641-773, Korea.
(e-mail: dhbae@sarim.changwon.ac.kr)
- Jun-Seok Chung and Won-Tae Kwon, Meteorological Research Institute, 460-18 Shindaebang-Dong, Dongjak-Gu, Seoul, 151-742, Korea.
- (Received September 1, 1999; revised October 2, 1999; accepted November 1, 1999.)